Smart Setup and Accelerometer Mounting Check for Vibration Measurements

Bin Liu
Product Manager, Brüel & Kjær Sound & Vibration Measurement A/S, Skodsborgvej 307, 2850 Nærum, Denmark
bin.liu@bksv.com

Dmitri Tcherniak
Research Engineer, Brüel & Kjær Sound & Vibration Measurement A/S, Skodsborgvej 307, 2850 Nærum, Denmark
dmitri.tcherniak@bksv.com

Niels-Jørgen Jacobsen
Product Manager, Brüel & Kjær Sound & Vibration Measurement A/S, Skodsborgvej 307, 2850 Nærum, Denmark
niels-jorgen.jacobsen@bksv.com

Martin Qvist Olsen
Product Manager, Brüel & Kjær Sound & Vibration Measurement A/S, Skodsborgvej 307, 2850 Nærum, Denmark
martinqvist.olsen@bksv.com

ABSTRACT

This paper describes some of the challenges experienced by many experimentalists and presents new ways of overcoming these. The Smart Setup can dramatically reduce the time required for the test setup and the presented Accelerometer Mounting Check procedure can check the transducer's health and the integrity of the whole measurement channel. The goal is to get the data right first time and in the shortest possible time.

Keywords: vibration measurement, smart setup, system verification, transducer mounting

1. Introduction

Performing vibration measurements can be quite time-consuming. In particular, proper mounting of transducers on the test structure, connecting them to the measurement hardware and checking everything is working as expected can be a significant part of the total test time. In addition, this often has to be done under extreme time constraints.

Obviously, not only large scale testing like modal surveys with hundreds of channels, but also smaller scaled tests, can benefit greatly from efficient measurement setup and system verification tools. Ensuring the integrity of each measurement channel becomes even more critical and difficult when transducers are located in remote areas or areas with limited or no access.

This paper first presents the technical background and the implementation of the patented technology called Accelerometer Mounting Check that can secure the health of all channels before and during measurements. Then Smart Setup, the patent-pending technology that can reduce measurement setup time, is introduced. A vibration measurement setup is used to illustrate the entire workflow.

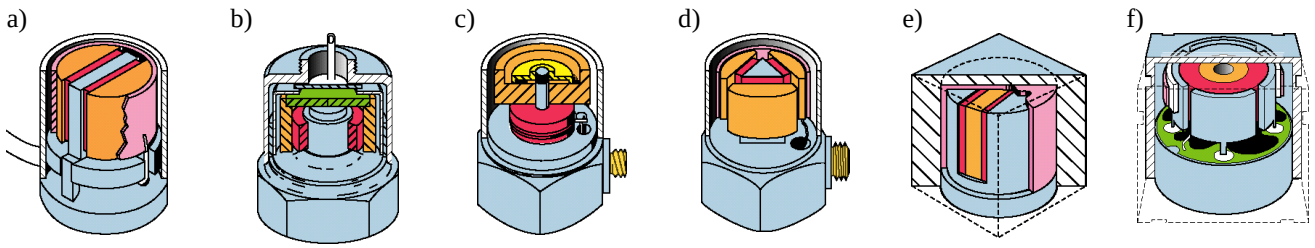

Fig. 1. Different designs of piezoelectric accelerometers: a) PlanarShear; b) annular shear; c) centre-mounted compression; d) DELTASHEAR®; e) THETASHEAR®; f) ORTHOSHEAR®.

2. Technical background

Typical designs of piezoelectric accelerometer are shown in **Fig. 1**. They all have a similar mechanical principal: the active part of such an accelerometer is one or several piezoelectric elements that together, act as a spring connecting the base of the accelerometer to the seismic mass. When the base is mounted on a test object, its vibrations are transmitted via the accelerometer mount to the base and further to the seismic mass. The force acting on the piezoelectric elements produces a charge proportional to the force acting on it and hence, the acceleration of the seismic mass. Over the operational frequency range, the seismic mass vibrates with the same magnitude and phase as the accelerometer base and the surface on which the accelerometer is mounted [1], and the charge output of the accelerometer correctly reflects the acceleration of the test object.

The direct piezoelectric effect utilized in the accelerometers is a reversible process, that is, the same piezoelectric material exhibits the reverse effect: responding to the applied electrical field, it generates an internal mechanical strain. Applied to the mechanical scheme implemented in the accelerometer, it means that subjecting the piezoelectric element with an alternating electric field, one will generate an alternating force acting on the seismic mass and the base. This force will be transmitted via the accelerometer structure and the accelerometer mount to the test object.

If the accelerometer's output is measured simultaneously with applying the excitation voltage, one can notice that the readings are sensitive to the implementation of the accelerometer mount. This sensitivity is utilized in the Accelerometer Mounting Check technology.

Let us demonstrate the mechanical concept behind the Mounting Check on a simple model. The mechanical parts of the accelerometer, the mount and the test object are modelled as a three degree-of-freedom system (**Fig. 2**). The seismic mass and the accelerometer body, represented by masses m_S and m_B respectively, are connected by the piezoelectric element represented by a spring with linear stiffness k_{PZ}. The mount is modelled as the second linear spring with stiffness k_M, attached to the test object. Mass m_D models the part of the structure, which is involved in the local mechanical vibration of the accelerometer-structure assembly. The forces caused by applying the electric excitation to the piezoelectric element are denoted as F. By

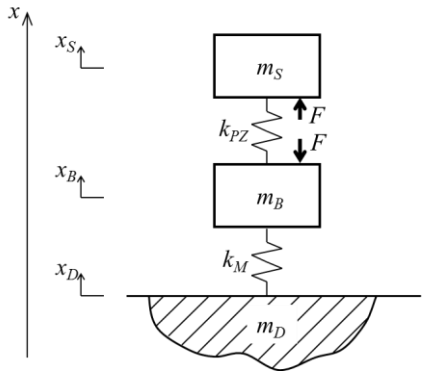

Fig. 2. Mechanical system representing the parts of the accelerometer and its mounting.

a)

b)

c)

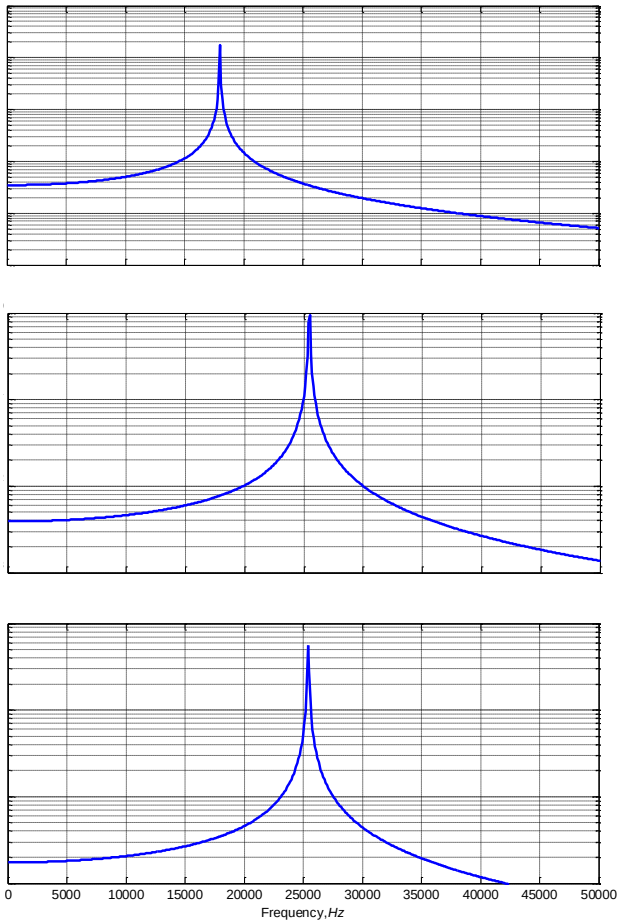

Fig. 3. Typical FRF $H(\omega) = s_0(\omega)/F_0$ for a) perfectly mounted on an infinitely heavy object; b) free hanging position; c) mounted on a light structure.

varying the parameters, one can observe how the accelerometer mounting (or the absence of mounting) affects the output of the accelerometer.

The equations of motion can be readily set

$$\begin{pmatrix} m_S & 0 & 0 \\ 0 & m_B & 0 \\ 0 & 0 & m_D \end{pmatrix} \begin{pmatrix} \ddot{x}_S \\ \ddot{x}_B \\ \ddot{x}_D \end{pmatrix} + \begin{pmatrix} k_{PZ} & -k_{PZ} & 0 \\ -k_{PZ} & k_{PZ} + k_M & -k_M \\ 0 & -k_M & k_M \end{pmatrix} \begin{pmatrix} x_S \\ x_B \\ x_D \end{pmatrix} = \begin{pmatrix} F \\ -F \\ 0 \end{pmatrix}. \quad (1)$$

Assuming harmonic excitation $F = F_0 e^{i\omega t}$ and steady state of the system, the equations of motion can be solved. The electric output of the accelerometer is proportional to the forces acting on the piezoelectric element, which are proportional to its deformation $s = x_S - x_B$. The latter can be presented in the form $s(t) = s_0(\omega)e^{i\omega t}, s_0 \in \mathbb{C}$, and the expression for the frequency response function (FRF) $H(\omega) = s_0(\omega)/F_0$ can be found analytically or evaluated numerically.

Fig. 3. shows typical FRFs for three limit cases: the accelerometer is perfectly mounted on infinitely heavy structure ($k_M \to \infty, m_D \to \infty$), the accelerometer is freely hanging $k_M = 0$ and the accelerometer is perfectly mounted on a very light structure ($k_M \to \infty, m_D \to 0$). The other parameters are set to the values typical to miniature Brüel & Kjær accelerometer Type 4507-C.

From the equation of motion (1), one can also obtain the values for the resonances frequencies. For the limit cases, they can be obtained from simple expressions [1]: For the accelerometer perfectly mounted on an infinite mass, the value of the *mounted resonance frequency* is

$$\omega_{MR}^2 = \frac{k_{PZ}}{m_S} \tag{2}$$

and in *free hanging position*, the resonance frequency is

$$\omega_{FH}^2 = k_{PZ}\left(\frac{1}{m_S} + \frac{1}{m_B}\right) \tag{3}$$

These values coincide with the frequency of the peaks in **Fig. 3a** and **Fig. 3b** respectively. For a typical case when $m_S \approx m_B$, the resonance frequency in free hanging position is about 40% higher than the mounted resonance frequency: $\omega_{FH} \approx \sqrt{2}\,\omega_{MR}$.

The above mentioned considerations demonstrate that it is possible to evaluate the state of accelerometer mounting based on the FRF estimated in the range between the mounted resonance frequency and the resonance frequency in free hanging position. Thus, if one could measure the FRF in this frequency range, it would be possible to judge if the accelerometer is properly mounted on the structure or if it would fall off.

3. Implementation

In brief, Accelerometer Mounting Check technology means sending an electrical excitation signal to accelerometer's piezoelectric element combined with simultaneous measurement of its response[1]. The practical implementation of the technology in industrial products involves a tight interaction between the data acquisition hardware and post-processing software. Let's take Brüel & Kjær LAN-XI modules and PULSE Reflex® software as an example.

3.1. FRF measurement

In practice, the FRF measurement consists of a number of steps:

1. PULSE Reflex® sends the connected LAN-XI data acquisition module(s) a command to start the Accelerometer Mounting Check test.
2. The LAN-XI module, using the built-in signal generator, generates a number of sine sweeps and sends them to the accelerometer; the sine sweeps are generated around the resonance frequency in free hanging position.
3. Simultaneously, the module measures the accelerometer response and sends the digitized data accompanied with the "sweep start" trigger events to PULSE Reflex®.
4. Knowing the chirp characteristics (the start and stop frequencies and the sweep rate), the software reconstructs the sine sweep signals that were employed for exciting the accelerometer. Using the reconstructed signal and the measured response, it calculates the FRF and coherence functions. The noise is attenuated by means of averaging.
5. PULSE Reflex® sends the LAN-XI module a command to end the Mounting Check test.
6. The resulting FRF and coherence function are used as a *characteristic* of the current mounting state.

The FRFs show in **Fig. 3** are based on analytical expression and a simplified accelerometer-mount-structure model. In reality, the construction of the accelerometer is much more advanced (**Fig. 1**), and the test object and the accelerometer mount cannot be generally represented as a simple mass-string system. Therefore, the real FRF corresponding to the perfectly mounted accelerometer may significantly differ from the analytical one shown in **Fig. 3**a. Examples of the measured FRFs corresponding to different structures and mounting schemes are shown in **Fig. 4**.

3.2. Detection of faulty mounts

The algorithm behind the Accelerometer Mounting Check technology will say whether the accelerometer is properly mounted on the structure or not, with a simple Yes or No. In *Machine learning* [2], such class of algorithms is called *Classification* or *Decision making*. In broad terms, the Machine learning suggests two ways of implementation: *unsupervised learning* and *supervised learning.*

The *unsupervised learning* may involve some parametric modelling of the FRF corresponding to the proper mounting (for example, using modal parameters). Then the classification will compare the model of the current state with the reference model of the proper mounting state. The deviations will indicate that the accelerometer is not properly mounted. The implementation of this approach might be difficult since the FRFs corresponding to the proper mounting state may significantly differ, depending on the test object and the mounting techniques (for example, compare the thick curves on **Fig. 4**). Then the opposite

[1] Patented technology

approach can be taken: comparing the thin curves in **Fig. 4**, one can notice that the FRFs corresponding to the improper mounting are very similar, and thus, using the improper state as the reference can be more sensible. Then, if the current state is different from the reference state, the mounting is good, and if the current state is close to the reference state, the mounting is bad.

In the case of the *supervised learning*, every time we mount the accelerometer on the structure, we measure and store the reference state. During the measurement campaign, we measure the current state and compare it with the reference state. The difference in the states indicates that something has happened with the mounting and it needs be checked.

The present Accelerometer Mounting Check implementation utilizes the supervised learning. For the user of the system, it involves the following steps:

1. The user mounts the accelerometers on the test object and connects them to the data acquisition modules.
2. When the process is completed, the user makes sure that all accelerometers are mounted correctly.
3. The Mounting Check "Create reference" procedure is started via PULSE Reflex® GUI. Internally, this procedure involves the number of steps described in section 3.1 but it is initiated by a single command (mouse-click). Then the "reference state" (consisting of the FRF and coherence curves), reflecting the correctly mounted accelerometers, is stored.
4. The user starts the measurements. Once in a while, between the tests, the user initiates the "Check mounting" procedure, which is called via PULSE Reflex® GUI. This procedure involves exactly the same steps as described above (see section 3.1).
5. The FRF and coherence curves generated in the last step are compared with those of the reference state. If the current and reference states differ significantly, the software informs the user about the potential problem with the accelerometer mounting, providing the information where the accelerometer is mounted (for example, its DOF or its location in setup geometry, if available). If the current state does not differ from the reference state, the system informs the user that all accelerometers are mounted correctly.

3.3. Classification algorithm

As mentioned earlier, the Accelerometer Mounting Check is implemented via a classification algorithm with supervised leaning. Depending on the mounting state, the classifier puts the samples into two classes: (i) "Proper mounting" and (ii) "Improper mounting". The classifier uses *features*, which is a reduced set of relevant parameters characterizing the class. To make the algorithm more robust to noise, we use two features. The first feature characterizes the difference between the reference FRF and the current FRF; this is a normalized scalar product of two FRFs' magnitude weighted by the corresponding coherence values:

$$f_1 = \frac{\sum_{\omega_1}^{\omega_2} \gamma_R^2(\omega)\gamma_C^2(\omega)\,|H_R(\omega)||H_C(\omega)|}{\sum_{\omega_1}^{\omega_2} |H_R(\omega)| \sum_{\omega_1}^{\omega_2} |H_C(\omega)|} \tag{4}$$

where the subscripts *R* and *C* denote the reference and current states respectively, $\gamma^2(\omega)$ is the coherence function and $[\omega_1;\ \omega_2]$ is the frequency range of interest. The second feature is the coherence index:

$$f_2 = \frac{1}{N} \sum_{\omega=\omega_1}^{\omega_2} \gamma_C^2(\omega) \tag{5}$$

where *N* is the number of frequency lines in the $[\omega_1;\ \omega_2]$ range. As one can notice, $f_1, f_2 \in [0; 1]$.

Each state of the system can be presented as a point in the features space. For the two features' classification problem, the state is a point with coordinates f_1 and f_2 (**Fig. 5**) on the (f_1, f_2) coordinate plane. Collecting several points representing the proper and improper mounting states, two clusters will be formed, in **Fig. 5** they are colored green and red respectively. A linear classifier can be presented as a line separating the clusters; the equation of the line on the (f_1, f_2) coordinate plane is $w_1 f_1 + w_2 f_2 + w_3 = 0$. The coefficients $w_1 \ldots w_3$ can be found experimentally, and they are invariant to the type of accelerometer, the mounting method and the test structure. The distance *d* between the point with coordinates (f_1, f_2) and the line is calculated as $d = w_1 f_1 + w_2 f_2 + w_3$. If $d > 0$, the point is below the separation line and represents the proper mounting. In contrast, the points with $d < 0$ are classified as belonging to the "Improper mounting" class. If the point is too close to the separation line, $|d| < \epsilon$, it can be classified as uncertain.

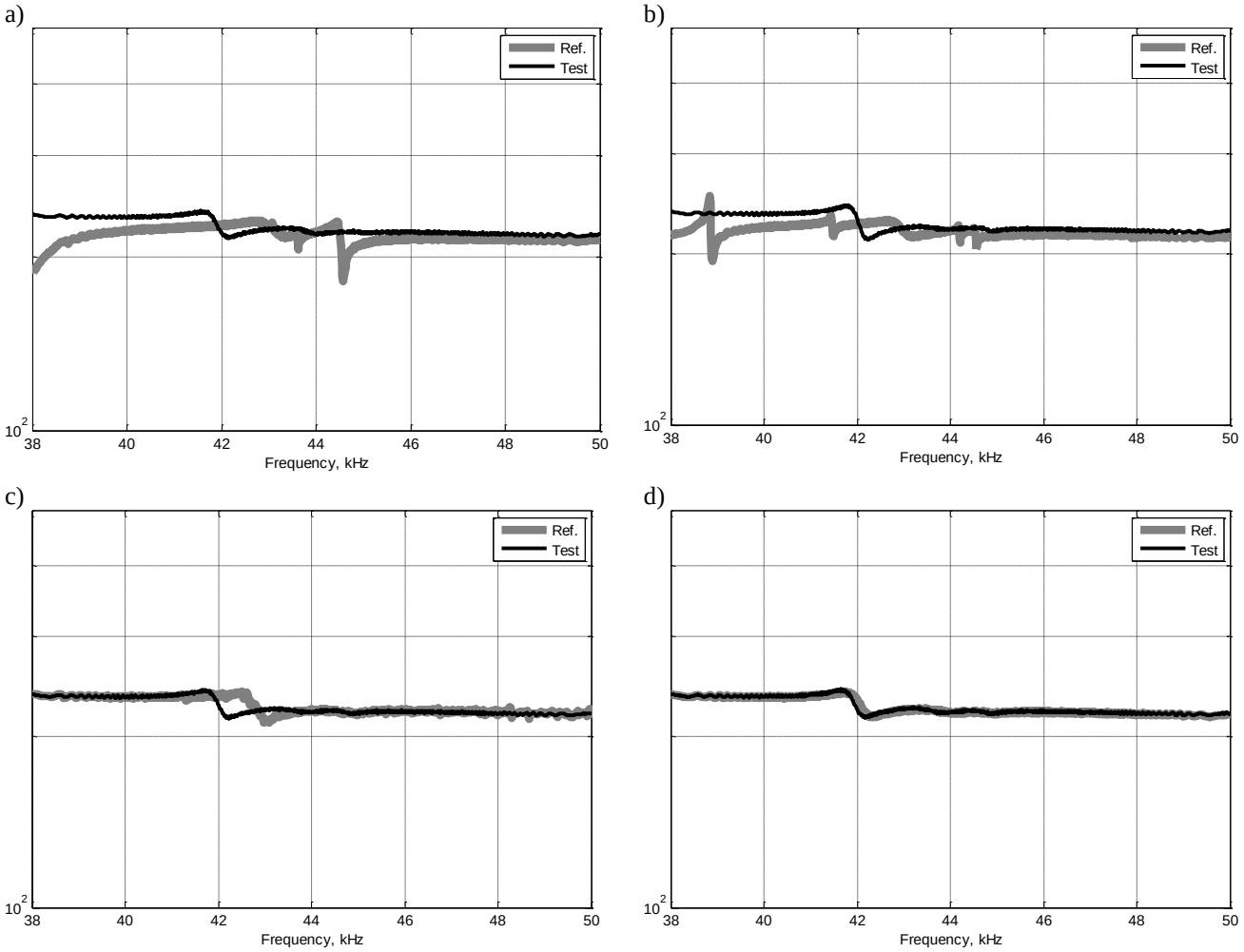

Fig. 4. FRFs. Thick grey: proper mount; thin black: the accelerometer falls off the structure. a) heavy steel block, steel stub; b) heavy steel block, beeswax; c) 1.5 mm steel plate, beeswax; d) composite structure (thickness 20 mm), beeswax.

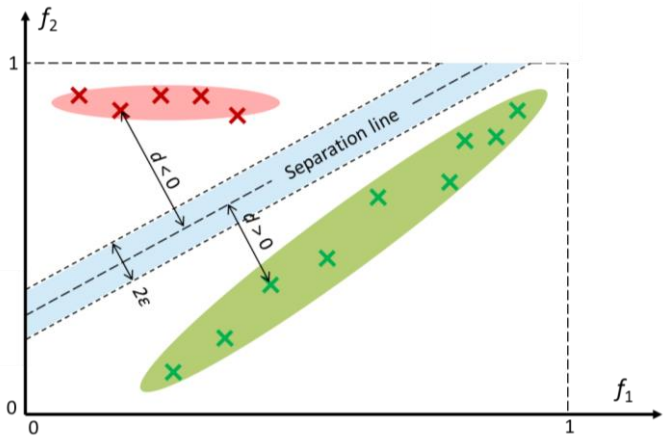

Fig. 5. Schematic view of the two features' space. Green crosses: the states representing the proper mounting, red crosses correspond to the states with improper mounting. Linear classification is represented by the separation line.

4. Smart Setup

When making measurements, it is often a challenge to align the degrees of freedom (DOF) information (Component ID, Node ID and DOF Direction) for transducer placement on the test object with the measurement software. Entering type numbers, serial numbers and transducer placement information manually into the measurement software is time-consuming and error prone.

The smart transducer setup scans the Data Matrix Code engraved on the transducer using the Transducer Smart Setup app available for IOS devices (iPhone, iPad and iPod touch) on iTunes (**Fig. 6**). This helps eliminate the time-consuming manual processes to mount transducers. It also keeps track of the mounted transducers in the data acquisition process.

Data Matrix Codes use Reed-Solomon error correction codes for reliable reading, regardless of scratching or denting from regular use of the accelerometer. The matrix codes can be generated to be used to encode DOF information (location and ID number) for the test setup.

The Transducer Smart Setup app helps register the DOF information correctly and enriches this with transducer metadata. The information can be loaded into PULSE Reflex to simplify setting up the data acquisition and analysis tasks. The Smart Setup smartphone app has a patented algorithm that automatically detects the orientation of an accelerometer by scanning the code, making sure that the transducer is synchronized with PULSE Reflex for faster setup and easier measuring.

Even without the app, one can scan the data matrix code with any 2D barcode scanner and get immediate access to detailed transducer information, including calibration data.

5.Vibration measurements

For every vibration measurement, proper mounting of transducers on the test structure, connecting them to the measurement hardware and checking that everything is working as expected, is time-consuming. When measuring on a big structure requiring a multichannel test system, it is even more crucial to do the above steps properly because the correct data must be acquired first time.

The test object with mounted accelerometers is shown in **Fig. 7**. In total, 25 triaxial CCLD accelerometers are used. A triaxial accelerometer, engraved with Data Matrix code on three surfaces, is shown in **Fig. 8**a. The codes engraved on the different surfaces are different, and each code indicates the measurement direction. The data matrix code printed on the sticker contains DOF information including location and node number, which are predefined by the user. **Fig. 8**b shows the scanning of the code using a mobile phone.

When the transducers are mounted with the help of Smart Setup, Accelerometer Mounting Check can help to ensure that the mounted accelerometers are mounted correctly following the procedure described in section 3.2.

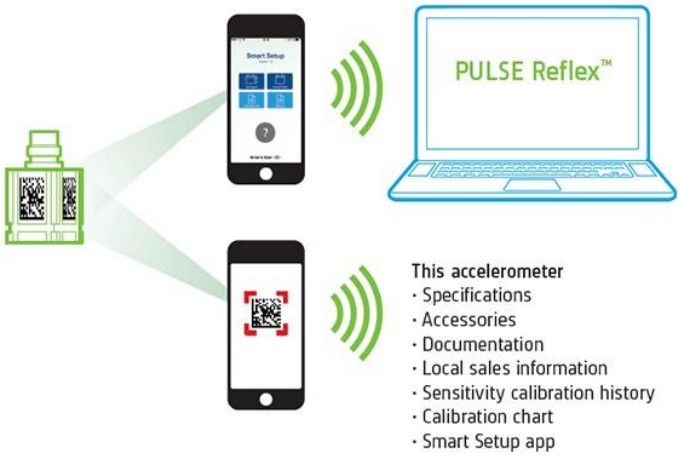

Fig. 6. Illustration of Smart Setup workflow.

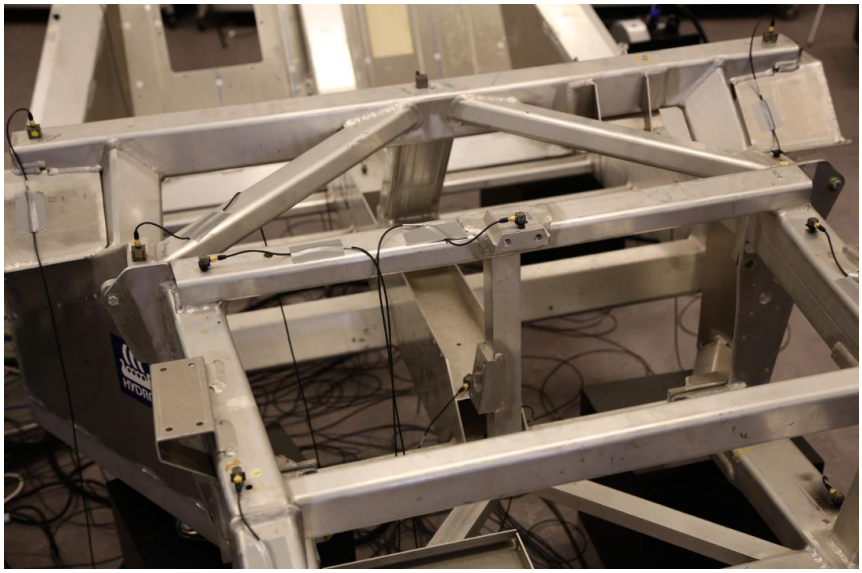

Fig. 7. Test object with accelerometers mounted

a) b)

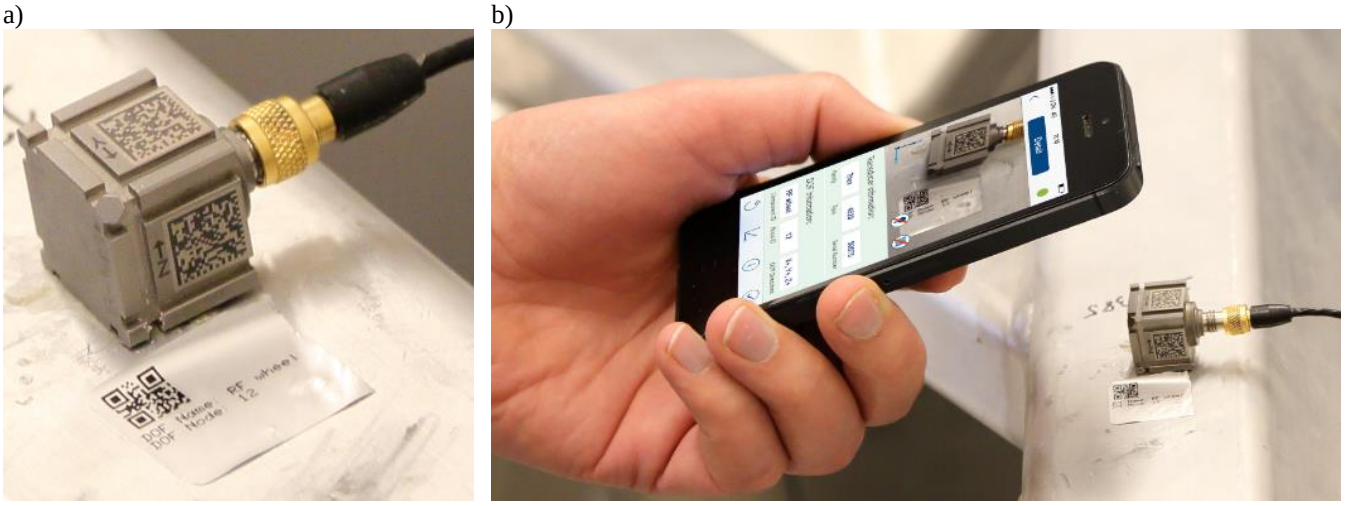

Fig. 8. a) Accelerometer with engraved Data Matrix Code; b) Scanning the Data Matrix Code using the Transducer Smart Setup app

6. Conclusion

The paper presents two innovative methods of efficiently conducting vibration measurements. Smart Setup, using the Data Matrix Code and an easily selected measurement coordinate system, reduces the setup time. Accelerometer Mounting Check ensures the health of all channels before and during measurements.

References

[1] M. Serridge and T. R. Licht, Piezoelectric accelerometers and vibration preamplifier handbook, Glostrup, Denmark: K.Larsen & Søn A/S, 1987.

[2] C. M. Bishop, Pattern recognition and machine learning, New York, USA: Springer, 2006.